JOURNAL OF STRUCTURAL ENGINEERING Vol.39 A (March 1993) JSCE

MECHANICAL PROPERTIES OF TUBULAR MEMBERS UNDER CYCLIC AXIAL LOADS

Yukio UEDA*, Hidekazu MURAKAWA** and Raafat El-Sayed SHAKER***

In this paper, the behavior of pin-ended tubular steel members under cyclic axial loads is studied. Twenty six models are analyzed utilizing the Finite Element Method (FEM) considering both geometrical and material non- linearities. The parameters considered in this study are the cyclic loading characteristics (strain amplitude and mean strain), geometrical parameters (diameter-to-thickness ratio D/t and normalized slenderness ratio λ) and material inelastic characteristics. The results of numerical analysis are closely examined with respect to both ultimate strength and energy dissipation capacity.

1. Introduction

Tubular members are used commonly in space trusses and offshore structures. Such structures are highly redundant, and failure of an individual member does not necessarily lead to an overall structural collapse but merely causes a redistribution of forces among members in the neighboring regions. The locally failed member may be capable of sustaining reduced load according to its own post-buckling characteristics. The nature of the post buckling curves dictates the manner in which load is shed to adjacent members. Overall collapse of the structure occurs when the redistributed load can not be sustained any further by the structure [1].

On the other hand, the offshore structures which are subjected to the extreme environmental loadings such as earthquake, wave and wind are normally designed considering their ultimate strength. In nature, these loadings are repetitive, therefore, the structures and their individual members must have a sufficient strength and ductility under cyclic loads. To predict the performance under extreme seismic loading conditions, it is necessary to investigate the inelastic cyclic behavior of the structures as well as their individual members. This has been the subject of intensive investigations in recent years [1)-6)].

A literature survey indicated that there is a lack of informations concerning the influence of the parameters affecting the hysteresis of the tubular members under cyclic loads. To investigate the behavior of tubular members under the inelastic cyclic loads, the effect of the following parameters must be studied:

i Geometrical parameters of the member (e.g. diameter to thickness ratio D/t and slenderness ratio λ)

ii Material inelastic characteristics (e.g. stress-strain curve , strain hardening and Bauschinger effects)

iii The end conditions of the member (e.g. simply supported, fixed and elastic support)

* Dr., Professor, Welding Research Institute, Osaka University, 11-1, Mihogaoka, Ibaraki, Osaka 567, Japan
** Ph.D., Assoc. Prof., Welding Research Institute, Osaka Univ, 11-1, Mihogaoka, Ibaraki, Osaka 567, Japan
*** Graduate Student, Osaka Univ, 11-1, Mihogaoka, Ibaraki, Osaka 567, Japan

IV The load conditions such as:

Proportional loads (e.g. cyclic axial load with or without eccentricity and cyclic bending)

Non-proportional loads (e.g. constant axial or lateral loads with cyclic bending)

V Cyclic loading characteristics (e.g. strain amplitude, mean strain and load or displacement control)

VI Initial imperfections (e.g. initial deflection and residual stresses)

In this paper, a qualitative study on the effect of the geometrical parameters, cyclic loading characteristics as well as the material inelastic characteristics on the behavior of pin-ended tubular member under cyclic axial loads is presented. The other end conditions and load conditions will be considered in the future work. Elasto-plastic large deformation analysis utilizing the Finite Element Method (FEM) was employed in this study. At first, the validity of the FEM code for the analysis of pin-ended tubular member under monotonically increasing load was examined through the comparison with an available published experimental data. Then, series of numerical analyses were performed to study the effects of the above mentioned parameters. Based on the numerical results, the influence of each parameter on the characteristics of pin-ended tubular member under cyclic axial loads was discussed.

2. Method of Analysis

2.1 Elasto-plastic large deformation analysis

In order to predict the inelastic behavior of individual tubular member, nonlinear Finite Element Method considering material and geometrical nonlinearities was used in this study. Since the accuracy of the Finite Element analysis depends greatly on the material models that describe the inelastic material behavior under cyclic loading conditions, the Finite Element code has been developed for different hardening laws, i.e, Elastic-Perfect Plastic, Isotropic, Kinematic and Mixed hardening rules.[7),8)]. A special isoparametric solid element with eight nodal points was utilized in the code following the formulations in the reference[9)].

2.2 Validation of the Finite Element code

To prove the applicability of the code to the Elasto-Plastic large deformation analysis of tubular member, one comparison was made on pin-ended tubular member under monotonically increasing axial loads. Table 1 gives the details of numerical model used in the comparison with experimental one reported in the reference[10)]. Due to the symmetry conditions, a quarter of the tube was analyzed. The mesh division is shown in Fig.1.

Figure 2 compares the load-displacement curve for the numerical result with the experimental one. In the analysis, relatively sharp peak load appeared, while this was not observed in the experiment. This may be due to neglecting the residual stresses in the analysis. In the post buckling curve, the experimental result seems to have a little higher strength than the numerical one. This could be due to neglecting the strain hardening in the analysis. As shown by Fig. 2, satisfactory correlations of the calculated results with the experimental ones were observed.

Table 1 : Data Used For Comparison with Ref. [10]

Model	L (mm)	λ	E (kgf/mm^2)	σ_y (kgf/mm^2)	e/L
CC42	2250	0.949	20863.	34.18	0.001

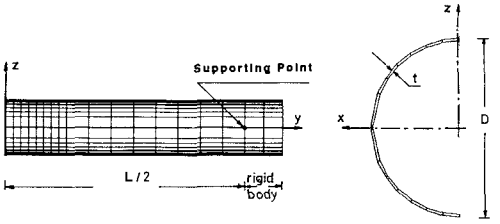

Fig. 1: Mesh Division

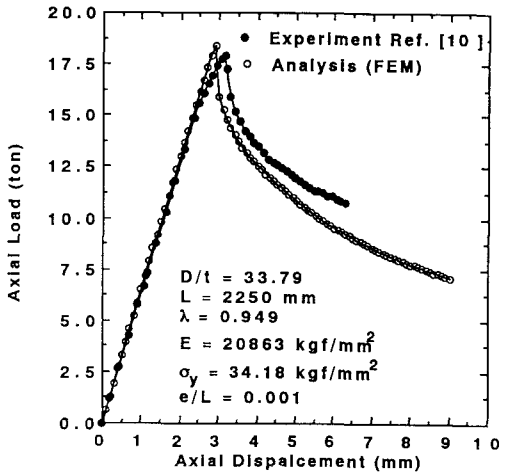

Fig. 2: Axial Force-Axial Displacement Curve

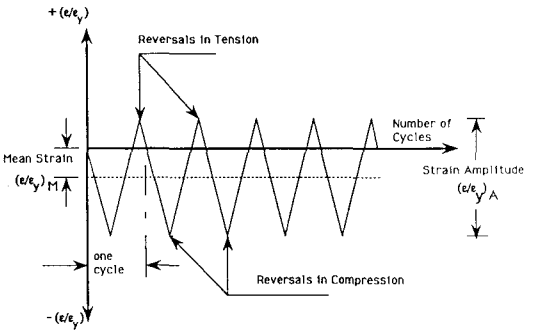

Fig. 3: Cyclic Loading Characteristics

2.3 Description of models and parameters

2.3.1 Numerical models

The numerical models investigated in this study were divided into three groups (L, G, M) according to the factor examined. All the models were axially loaded tubular members with pin end condition and subjected to eight load cycles starting from compression. The axial load was applied with eccentricity of one thousandth of the length L to initiate the buckling. Normalized parameters D/t and λ were chosen so that the influence of each parameter could be clarified. Table 2 lists the detailed data of numerical models used in this study. In the simulation, bilinear stress-strain relationship was assumed. The material properties used for calculation were as follows:

Yield stress: σ_y = 40 kgf/mm^2 Young's modulus: E = 21000. kgf/mm^2

From the symmetry conditions, a quarter of the tube was analyzed using the same mesh division as shown in Fig.1.

2.3.2 Cyclic loading characteristics

Idealized cyclic loading which is used in the analysis may be classified into two types, which are the cyclic loading with force control and with displacement control. In case of force control cyclic loading, the maximum applied loads should not exceed ultimate strengths. A typical example of applying this type of repetitive loads is the non-linear shakedown analysis of the structure to investigate whether the structure is likely to fail from the repetitive loads, or the structure remains stable[11]. On the other hand, when the member/structure is subjected to a severe cyclic loading caused by earthquake, the cyclic loadings with displacement control are often used in the analysis. Thus, to predict the behavior of the tubular member under severe load reversals in the inelastic regime, the cyclic loading with displacement control were applied in this study. This type of cyclic loading can be characterized by two parameters, which are the strain amplitude, $(\varepsilon/\varepsilon_y)_A$, and the mean strain, $(\varepsilon/\varepsilon_y)_M$. Figure 3 shows a typical example of regular cyclic loading with displacement control and its parameters.

3. Result of Numerical Analyses and Discussion

Table 2: *Description of the* Numerical Models and Parameters

Model	D/t	λ	L (mm)	e/L	Loading Characteristics			Material Properties				Parameter Examined
					$(\varepsilon/\varepsilon_y)_A$	$(\varepsilon/\varepsilon_y)_M$	number of cycles	σ_Y	E	E_T/E	hardening rule	
L4(+0)	72	.5	200	.001	4.0	0.0	8	40.	21000.	0.0	Elastic -perfect plastic	Cyclic Loading Characteristics
L6(+0)	72	.5	200	.001	6.0	0.0	8	40.	21000.	0.0	Elastic -perfect plastic	
L6(-1)	72	.5	200	.001	6.0	-1.0	8	40.	21000.	0.0	Elastic -perfect plastic	
L6(-2)	72	.5	200	.001	6.0	-2.0	8	40.	21000.	0.0	Elastic -perfect plastic	
L6(-3)	72	.5	200	.001	6.0	-3.0	8	40.	21000.	0.0	Elastic -perfect plastic	
L6(+3)	72	.5	200	.001	6.0	+3.0	8	40.	21000.	0.0	Elastic -perfect plastic	
G.337-24	24	.337	200	.001	4.0	-1.0	8	40.	21000.	0.0	Elastic -perfect plastic	Geometrical Parameters
G.337-36	36	.337	200	.001	4.0	-1.0	8	40.	21000.	0.0	Elastic -perfect plastic	
G.337-48	48	.337	200	.001	4.0	-1.0	8	40.	21000.	0.0	Elastic -perfect plastic	
G.337-60	60	.337	200	.001	4.0	-1.0	8	40.	21000.	0.0	Elastic -perfect plastic	
G.337-72	72	.337	200	.001	4.0	-1.0	8	40.	21000.	0.0	Elastic -perfect plastic	
G.5-24	24	.5	200	.001	4.0	-1.0	8	40.	21000.	0.0	Elastic -perfect plastic	
G.5-36	36	.5	200	.001	4.0	-1.0	8	40.	21000.	0.0	Elastic -perfect plastic	
G.5-48	48	.5	200	.001	4.0	-1.0	8	40.	21000.	0.0	Elastic -perfect plastic	
G.5-72	72	.5	200	.001	4.0	-1.0	8	40.	21000.	0.0	Elastic -perfect plastic	
G.85-24	24	.85	200	.001	4.0	-1.0	8	40.	21000.	0.0	Elastic -perfect plastic	
G.85-36	36	.85	200	.001	4.0	-1.0	8	40.	21000.	0.0	Elastic -perfect plastic	
G.85-48	48	.85	200	.001	4.0	-1.0	8	40.	21000.	0.0	Elastic -perfect plastic	
G.85-60	60	.85	200	.001	4.0	-1.0	8	40.	21000.	0.0	Elastic -perfect plastic	
G.85-72	72	.85	200	.001	4.0	-1.0	8	40.	21000.	0.0	Elastic -perfect plastic	
G.2-24	24	2.0	200	.001	4.0	-1.0	8	40.	21000.	0.0	Elastic -perfect plastic	
G.2-36	36	2.0	200	.001	4.0	-1.0	8	40.	21000.	0.0	Elastic -perfect plastic	
G.2-48	48	2.0	200	.001	4.0	-1.0	8	40.	21000.	0.0	Elastic -perfect plastic	
G.2-60	60	2.0	200	.001	4.0	-1.0	8	40.	21000	0.0	Elastic -perfect plastic	
MA60P	72	.337	200	.001	4.0	-1.0	8	40.	21000	0.0	Elastic -perfect plastic	Material Inelastic Characteristics
MA60K	72	.337	200	.001	4.0	-1.0	8	40.	21000	1/20	Kinematic	

D = outer diameter, t = thickness of the tube, L = length (mm), σ_y = yield stress in kgf/mm^2

E = Young's modulus in kgf/mm^2 E_T = Plastic modulus

λ = normalized slenderness ratio = $\frac{L/r}{\pi\sqrt{E/\sigma_y}}$ r = radius of gyration

$(\varepsilon/\varepsilon_y)_A$ = normalized strain amplitude $(\varepsilon/\varepsilon_y)_M$ = normalized mean strain

e = eccentricity of the applied load

3.1 Fundamental behavior of tubular member under cyclic axial loads

Figure 4 shows the hysteresis loops of model G.5-72. The first stage O-A is elastic compressive loading of the column until the ultimate loading capacity is reached at point A. The stage A-B-C is characterized by a decreasing of the axial load with the increase of applied axial displacement. This is primarily due to the formation of a lateral deflection in the column which facilitates the formation of a plastic hinge caused by the axial load and the bending moment. After a hinge is formed, the longitudinal compressive plastic strain at the midspan is increased due to the increase of the bending moments. At point B , this plastic strain reaches a certain critical value and the local buckling starts in the wall of the cross section. This local buckling reduces the full plastic moment capacity of the cross section and accelerate the decrease of the compressive load carrying capacity of the column. The maximum distortion of the cross section and out of straightness of the column are reached in the end of the compressive loading, i.e. at point C. Stages C-D and D-E-F are, respectively, the elastic unloading and tensile loading of the column. The slope of the curve is less than that for stage O-A since the stiffness of a member with an initial deflection and/or local buckling is smaller than that for a virgin member. During the application of a tensile force of an increasing magnitude, the re-yielding takes place in the tension side. As the tensile load increases after re-yielding, the stiffness of the column (which is the slope of load-displacement curve), gradually decreases with spread of yielded zone due to the increases in tension and reversed bending. The stage F-G is the elastic unloading of the column under tensile force. The subsequent hysteresis loops for a cyclically loaded column have the same general characteristics, with the following changes:

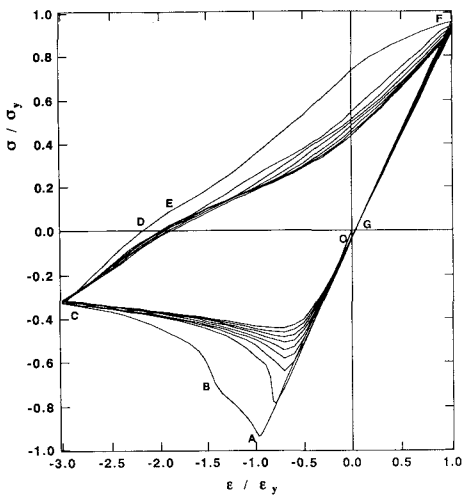

(a) Axial Force-Axial Displacement Loop

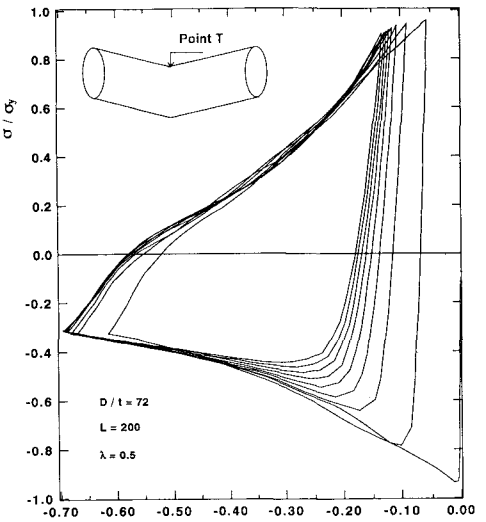

(b) Axial Force-Lateral deflection Loop

Fig. 4: Hysteretic Loops for model G.5-72

1) The starting point for a new hysteresis loop begins at the end of the preceding one. Thus, in Fig. 2 a point such as O is translated to G.
2) The consecutive peak compressive loads are reduced. Referring to Fig. 4-b, this is due to a residual deflection and/or local buckling in a member formed under compressive load.
3) The consecutive peak tensile loads, which follow compressive ones are also reduced. This may be attributed to the accumulated residual deflection and/or local buckling.
4) After eight cycles, however, the hysteresis loops tend to stabilize.

3.2 Parameters affecting hysteresis

Two criteria can be applied to evaluate the performance of the column under cyclic loading, namely the ultimate strengths, in both tension and compression, and the energy dissipation capacity. The energy dissipation capacity is defined as the average energy dissipated per unit volume. Further, its normalized value with respect to $\sigma_y \varepsilon_y$ is referred to as normalized energy dissipation which corresponds to the area under the normalized load-displacement curve, i.e

$$\int \sigma \, d\varepsilon / \sigma_y \varepsilon_y.$$

3.2.1 Effect of cyclic loading characteristics

In this section, seven models, belonging to group (L), were adopted in order to study the effect of cyclic loading characteristics such as strain amplitude; $(\varepsilon/\varepsilon_y)_A$; and mean strain; $(\varepsilon/\varepsilon_y)_M$; on the ultimate strengths and energy dissipation capacity of the tube. As listed in Table 2, the models of this group had the same diameter-thickness ratio (D/t = 72) , normalized slenderness ratio (λ = .5) and the material was assumed to be elastic-to-perfect plastic.

Figure 5 shows the effect of strain amplitude; $(\varepsilon/\varepsilon_y)_A$; on the deterioration of normalized ultimate tensile and compressive strengths with increasing number of cycles. This figure indicates that the rate of deterioration of both

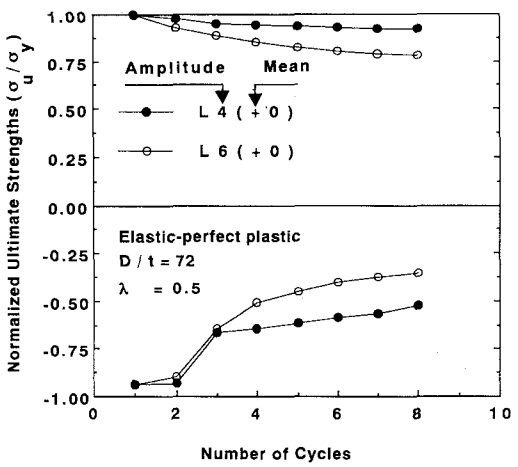

Fig. 5: Effect of Strain Amplitude on the Deterioration of the Ultimate Strengths

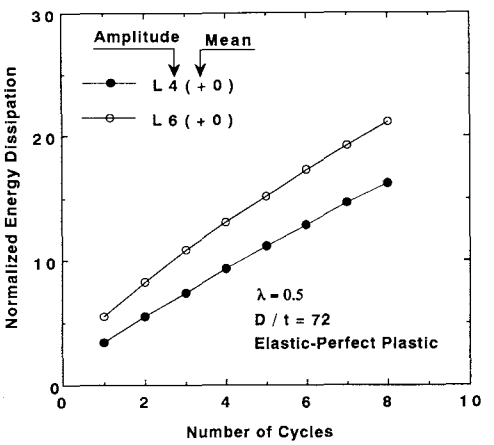

Fig. 6: Effect of Strain Amplitude on the Accumulated Energy Dissipation

ultimate strengths increases with the increase of the strain amplitude. This may be attributed to the fact that when the strain amplitude is large, the damage caused by the compressive loading becomes large. Also it can be seen that the ultimate compressive strength deteriorated at a faster rate than the ultimate tensile strength.

The effect of this parameter on the accumulated normalized energy dissipation capacity is illustrated in Fig. 6. As expected, the rate of increase of the energy dissipation capacity is not as large as that of strain amplitude. This is due to the fact that the load carrying capacity of the subsequent cycles is reduced when the strain amplitude is large.

The effect of mean strain; $(\varepsilon/\varepsilon_y)_M$; on the ultimate strengths in both directions is illustrated in Fig. 7. As this figure indicates, the shift of the mean strain toward the compressive loads reduces the compressive strength for the second cycle and the following few cycles significantly. However, after eight cycles, it seems that the shift of mean strain has a slight influence on the converged compressive ultimate strength.

Figure. 8 shows the accumulated normalized energy dissipation capacity versus the number of cycles for different values of mean strain. This figure indicates that increasing the shift of mean strain toward the compressive loads decreases the energy dissipation capacity. However, the shift of mean strain has no significant influence on the rate of accumulated normalized energy dissipation capacity, i.e. the slope of lines in the figure.

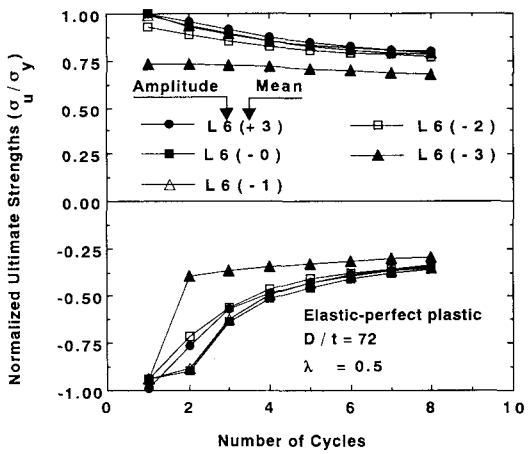

Fig. 7: Effect of Mean Strain on the Deterioration of the Ultimate Strengths

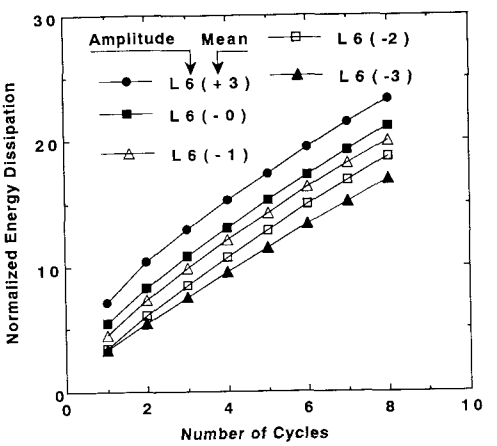

Fig. 8: Effect of Mean strain on the Accumulated Energy Dissipation

3.2.2 Effect of geometrical parameters, (D/t) and (λ)

Eighteen numerical models, belonging to group G, were chosen to investigate the effect of geometrical parameters (D/t, λ) on ultimate strengths and energy dissipation capacity of the tube. As summarized in Table 2, the models in this group were subjected to eight cycles starting from compressive loading with normalized strain amplitude of 4.0 and normalized mean strain of -1.0. The materials used in this group were assumed to be elastic-perfect plastic. At first, the failure modes are clarified to provide a better understanding of the effect of parameters examined in this section.

The global and local deflections of the tubular member at its midspan are plotted against the number of reversals in compression and tension in Figs.9, 10, 11 for three cases, namely short column (λ =0.337), medium column (λ =0.85) and long column (λ =2.0), respectively. The global deflection is defined as the average of the lateral displacements at top and bottom of the midsection. The local deflection is defined as the difference between them. In case of short columns, the local deflection is dominant under compression when D/t is large such as the case of D/t=72. The magnitude of the local deflection is increased with the number of cycles. As for the residual deformation after the application of tensile loading, the local deformation is relatively large when D/t=72. When the column has the intermediate length and large value of D/t, the global and the local deflections have the same order of magnitude under compression. In case of long columns, the global deflection is dominant under compression and the residual global deflection under tensile load is large when D/t is small. As Figs. 9, 10, and 11 indicate, the local buckling is the dominant mode of failure in the case of short columns with smaller λ such as .337. Meanwhile, in the case of long column with larger λ, such as 2.0, the dominant mode of failure is the global buckling.

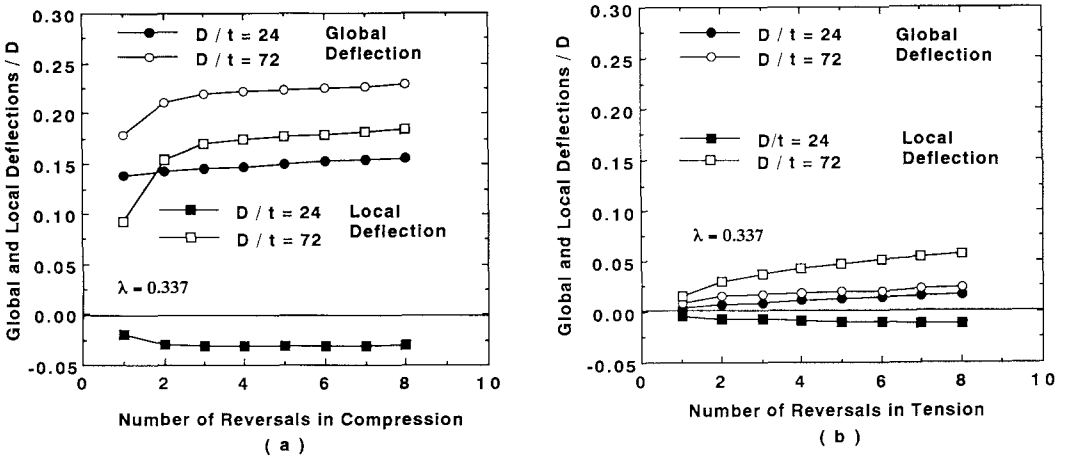

Fig. 9: Grouth of Global an Local Deflections Vs. Number of Reversals in Cases of λ = 0.337

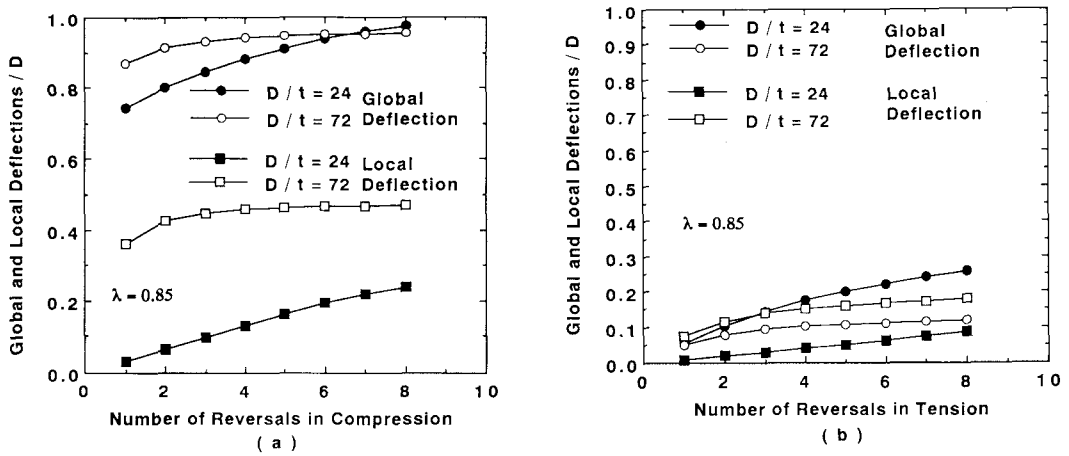

Fig. 10: Grouth of Global an Local Deflections Vs. Number of Reversals in Cases of λ = 0.850

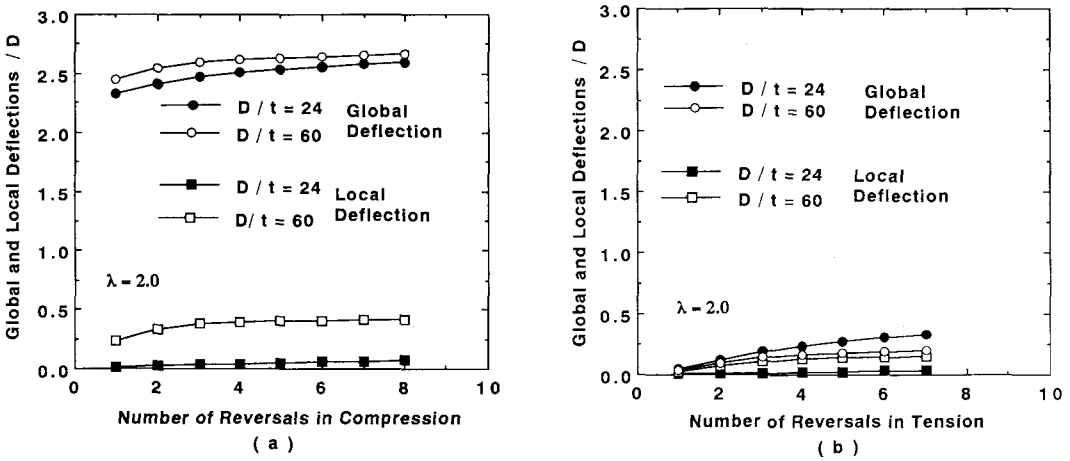

Fig. 11: Grouth of Global an Local Deflections Vs. Number of Reversals in Cases of $\lambda = 2.0$

Shown in Figs. 12,13, 14, 15 are the deterioration of normalized ultimate strengths versus number of cycles with different diameter-to-thickness ratios, D/t = 24 ~ 72 in cases of λ=.337, .5, .85, 2, respectively. In case of very short column such as λ=.337, it is observed that increasing D/t ratios has a slight influence on reducing the normalized ultimate strengths in the first few cycles. While, as the number of applied strain cycles increases, the compressive strength of the column is reduced significantly. This may be due to the accumulated local buckling. This local buckling reduces the full plastic moment of the cross section and consequently the compressive strength in the subsequent load cycles. In cases of larger λ such as .85 and 2.0, the effect of D/t on the compressive strength is small because the deformation is caused mostly by elastic buckling. Thus the lines in Fig. 15 almost coincide each other. However, the influence of D/t is observed in tensile strength when the column is long. This can be explained by the fact that the global deflection under tensile load is bigger when D/t is small as shown by Fig.11-b.

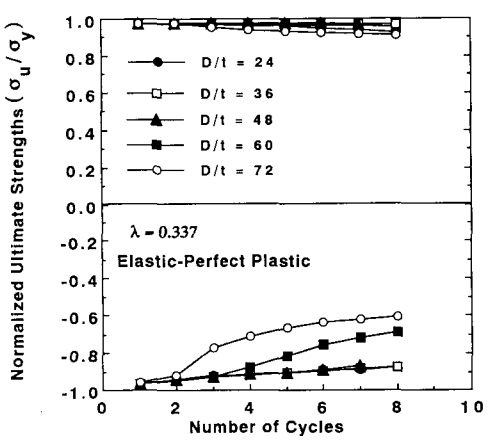

Fig. 12: Effect of D/t Ratios on the Deterioration of Ultimate Strengths in Cases of $\lambda = 0.337$

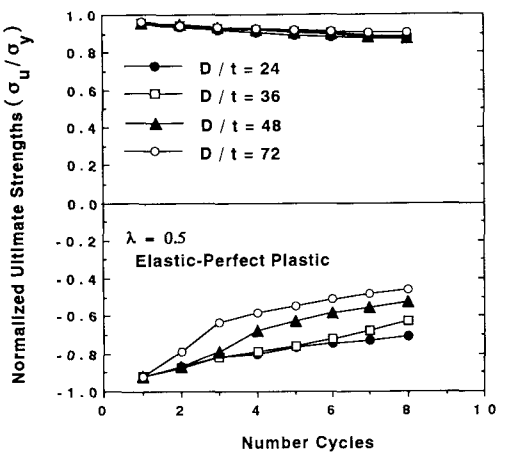

Fig. 13: Effect of D/t Ratios on the Deterioration of Ultimate Strengths in Cases of $\lambda = 0.5$

Generally, It can be seen that the largest deterioration after eight load cycles is observed in column with intermediate length (λ =.85) and fairly large deterioration in short columns (λ = .337 and 0.5). By comparing the compressive ultimate strength between the cases with D/t=24 and 72, as shown in Fig. 16, it is seen that the deterioration of the compressive ultimate strength in case of λ=.85 is caused by the accumulated global deflection, while in case of λ=.337 and .5, it is caused by the accumulated local buckling.

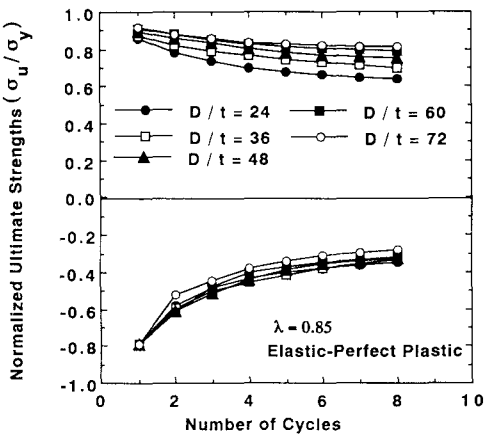

Fig. 14: Effect of D/t Ratios on the Deterioration of Ultimate Strengths in Cases of λ = 0.850

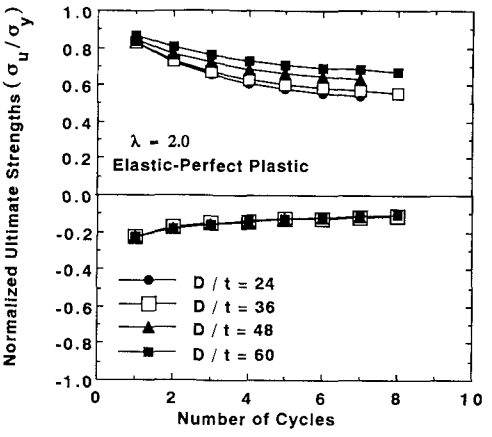

Fig. 15: Effect of D/t Ratios on the Deterioration of Ultimate Strengths in Cases of λ = 2.0

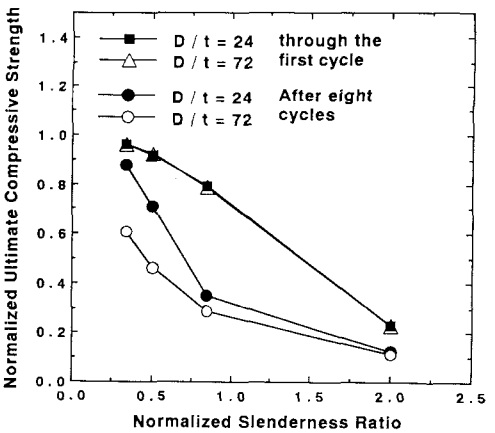

Fig. 16: Effect of Geometrical Parameters on the Detrioration of Ultimate Compressive Strength

Figures 17, 18, 19, 20 show the normalized accumulated energy dissipation versus number of cycles with different D/t ratios in cases of λ=.337,.5,.85,2. respectively. In case of λ=.337, as Fig.17 indicates , it can be observed that in the earlier cycles, the energy dissipation capacity is almost equal for all D/t ratios. However, in the subsequent cycles, increasing D/t ratio has a significant effect on reducing the accumulated energy dissipation capacity of the member. This may be attributed to the growth of local buckling which accelerates the reduction of the load carrying capacity in the inelastic regime. When the columns are long as in the case of λ=2.0, the effect of local buckling is small and the lines in Fig. 20 almost coincide each other.

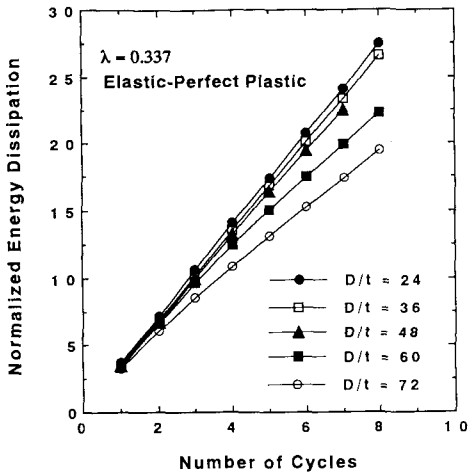

Fig. 17: Effect of D/t Ratios on the Accumulated Energy Dissipation in Cases of λ = 0.337

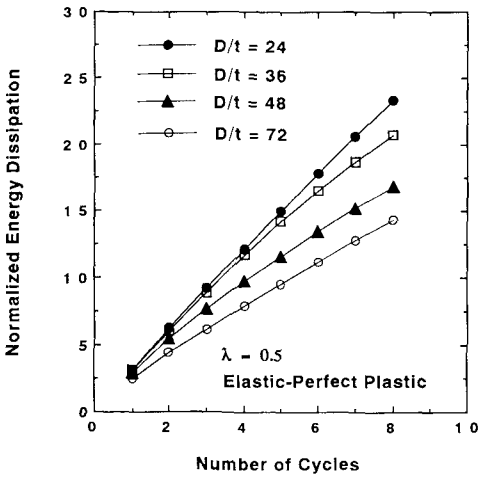

Fig. 18: Effect of D/t Ratios on the Accumulated Energy Dissipation in Cases of λ = 0.5

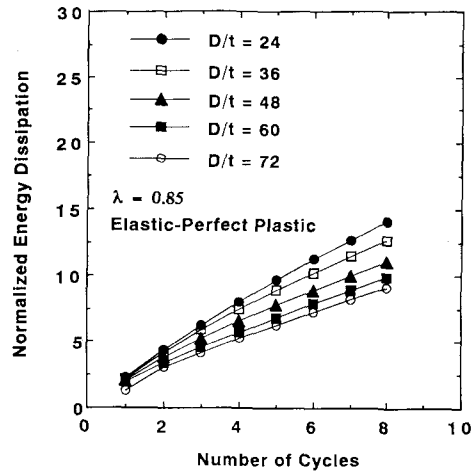

Fig. 19: Effect of D/t Ratios on the Accumulated Energy Dissipation in Cases of λ = 0.850

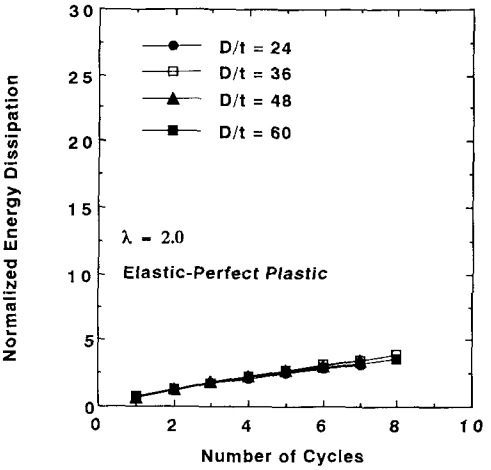

Fig. 20: Effect of D/t Ratios on the Accumulated Energy Dissipation in Cases of λ = 2.0

In general, it may be noticed that the accumulated energy dissipation capacity decreases with increase of λ, as shown in Fig. 21. Also, the effect of D/t ratios on the energy dissipation capacity decreases when λ is large. These could be explained by the fact that the mode of failure changes from local to global buckling when λ increases.

3.2.3 Effect of material inelastic characteristics

Two numerical models, belonging to group M, were selected to study the effect of material inelastic characteristics on the behavior of the tubular member under cyclic axial loads. In the simulation, a bilinear stress-strain curve was assumed and two constitutive laws were applied, namely the elastic-perfect plastic and kinematic strain hardening. As listed in Table 2, the two models in this group had the same (D/t) ratio of 72 and λ of .337 and

were subjected to eight cycles, starting from compressive loading, with normalized strain amplitude equal to 4.0 and normalized mean strain equal to -1.0.

Figure 22-a shows the deterioration of ultimate strengths for the two cases. This figure shows that, a significant reduction of the compressive strength is found in the case of the material without strain hardening. While it is not observed in the case of the material having strain hardening. This is due to the fact that strain hardening of material can contribute to reduce the concentration of the plastic strain at the midspan and consequently prevent the occurrence of local buckling, as shown by Fig. 22-b in which the development of local deflection with cyclic loading and the deformed midcross-sections of the columns are described.

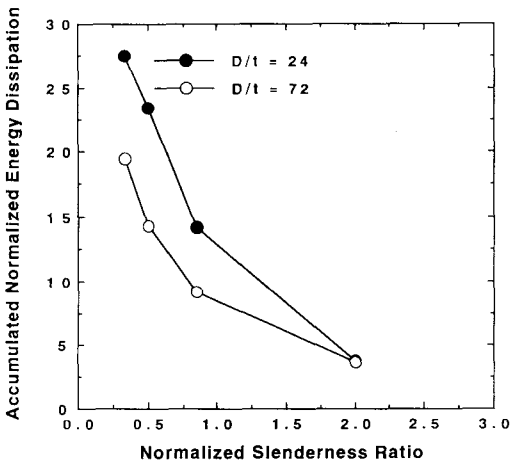

Fig. 21: Effect of Geometrical Parameters on the Accumulated Energy Dissipation after eight cycles

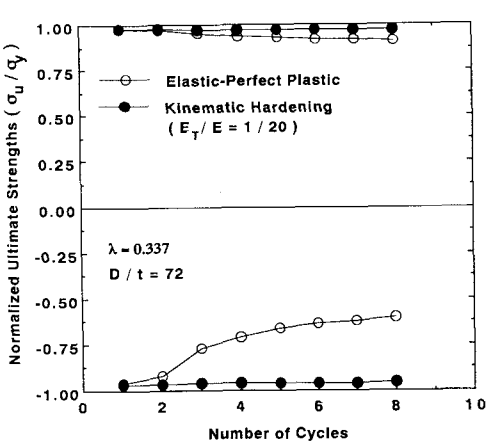

Fig. 22-a: Effect of Material Inelastic Characteristics on the Deterioration of Ultimate Strengths

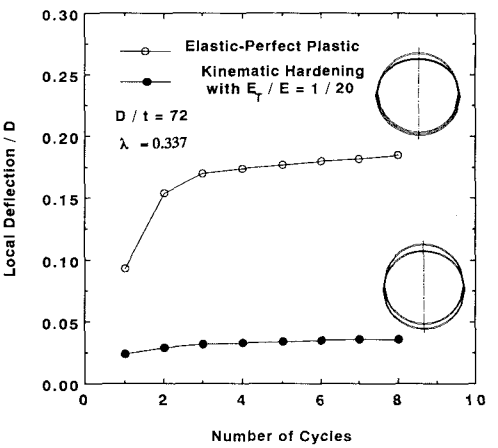

Fig. 22-b: The Grouth of the Local deflection Vs. Number of Reversals in Compression

Figure 23 shows the normalized accumulated energy dissipation for the two cases. It may be seen that, comparing with the elastic-perfect plastic model, kinematic strain hardening has a significant contribution in increasing the energy dissipation capacity of the member, particularly, when the number of applied strain cycle increases. This may be attributed to the strain hardening which prevents the occurrence of local buckling in the post ultimate regime and the reduction of the subsequent compressive strength.

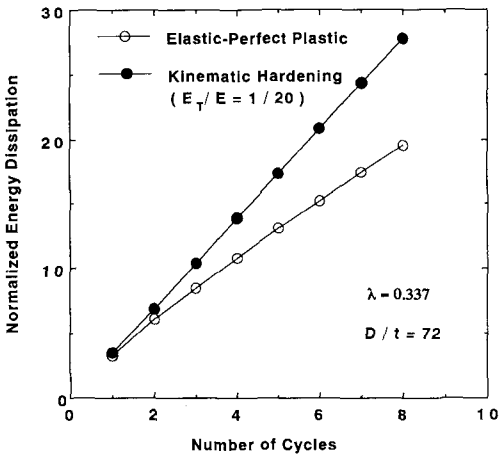

Fig. 23: Effect of Material Inelastic Characteristics on the Energy Dissipation

4. Concluding Remarks

The behavior of pin-ended tubular members under cyclic axial loads was investigated. Twenty six numerical computations were performed by utilizing the Finite Element Method considering both geometrical and material nonlinearities. The factors considered in this investigation were the cyclic loading characteristics, geometrical parameters and material inelastic characteristics. Based on the results of numerical analyses, the following conclusions were drawn;

(1) Increasing the strain amplitude has a significant influence on reducing the ultimate strengths as well as the magnitude of accumulated energy dissipation capacity of the column. Meanwhile, the shift of mean strain slightly influences the converged ultimate strengths and the energy dissipation capacity.

(2) For a short column with small λ and large D/t ratio, the local buckling becomes the significant mode of failure. Meanwhile, the global buckling becomes the significant mode of failure in case of long columns.

(3) For the pin-ended tubular member under cyclic axial loads , in general, the effect of the local buckling on the strength and energy dissipation capacity increases with an increase of D/t ratio and with a decrease of normalized slenderness ratio λ. For a member with D/t > 36, the effect of local buckling becomes significant. Therefore, the effect of local buckling must be considered in the design of thin tubular structures under severe cyclic loadings.

(4) It was found that the strain hardening is effective to prevent the local buckling under cyclic loading and the material having strain hardening are desirable from strength and energy dissipation capacity points of view.

References

1) Chen S. L. and Kitipornchai S. " Inelastic Post-Buckling Behavior of Tubular Structures". J. Struct. Engrg., ASCE, Vol. 114 (No.5) (1988), pp. 1091-1105.

2) Maison B. F. and Popov E. P."Cyclic Responce Prediction for Braced Steel Frames" J. Struct. Engrg. ASCE, Vol. 106(No.7) (1980), pp. 1401-1416.

3) Toma S. and Chen W. F."Inelastic Cyclic Analysis of Pin-Ended Tubes" J. Struct. Engrg. ASCE, Vol. 108 (No. 10)(1982), pp. 2279-2294.

4) Toma S. and Chen W. F. "Cyclic Inelastic Analysis of Tubular Column Section" Computers and Structures, Vol. 16(No. 6)(1983), pp. 707-716.

5) Sohal I. S. and Chen W. F. " Local Buckling and Inelastic Behavior of Tubular Sections" J. Thin-Walled Structures, Vol. 6(No. 1)(1988), pp. 63-80.

6) Yao T. and Nikolov P. I. " Numerical Experiment on Buckling/Plastic Collapse Behavior of Plates under Cyclic Loading"Prediction of Damage and Residual Strength of Tubular Member Under Collision". The US-JAPAN Joint Seminar on Stability and Ductility of Steel Structures Under Cyclic Loadings, Osaka (1992), Japan, CRC Press.

7) Ziegler H. " A modification of Prager's Hardening Rule". Quarterly of Applied Mathematics 17:55-65.

8) W. F. Chen and D. J. Han " Plasticity for Structural Engineers." Springer- verlag (1988).

9) Murakawa H. , Ueda Y. and Xiang D. " Prediction of Damage and Residual Strength of Tubular Member Under Collision". The US-JAPAN Joint Seminar on Stability and Ductility of Steel Structures Under Cyclic Loadings, Osaka (1992), Japan, CRC Press.

10) Rashed S. M. H., Katayama M., Isha H., Toda I., Oda K. and Yoshizaki T."Analysis of Non Linear and Collapse Behavior of TM Space Trusses" Third International Conference On Space Structures, 1984.

11) Hellaw O., Skallerud B., Amdahl J., Moan T."Reassessment of Offshore Steel Structures: Shakedown and Cyclic Non Linear FEM Analysis" The Proceeding of First International Offshore and Polar Engineering Conference, Vol. IV, 1991, pp. 34-42.

(Received September 21, 1992)